Kinetics and Mechanism of Degradation of a Cyclic Hexapeptide (Somatostatin Analogue) in Aqueous Solution

Ramesh Krishnamoorthy[1] and Ashim K. Mitra[1,2]

Received September 23, 1991; accepted February 21, 1992

A highly active cyclic hexapeptide analogue of somatostatin, Cyclo(*N*-Me-L-Ala-L-Tyr-D-Trp-L-Lys-L-Val-L-Phe), L-363,586, was found to improve the control of postprandial hyperglycemia in diabetic animals when given in combination with insulin. The compound is reported to be relatively stable in blood, nasal cavity, and intestinal lumen but undergoes rapid degradation in aqueous solution. The objective of this study was to elucidate the degradation mechanisms based on the kinetic data and the structure of the degradation products. Both pH and temperature had a profound influence on the instability of the peptide in aqueous solution. The data indicated that the peptide was most stable at a pH of about 4.7. The pH–rate profile exhibited specific acid catalysis at a pH less than 3.0 and base catalysis above pH 10.5. The kinetic pK_a was determined to be 9.7. This pK_a could be attributed to the tyrosine residue. The mechanisms of degradation under acidic and alkaline conditions appear to be different. Identification of the fragments obtained using mass spectrometry and amino acid sequencing suggest that the cyclic compound was cleaved to yield a linear fragment, which underwent further cleavage at both peptide linkages alpha to the tryptophanyl residue. The indole group of that residue is probably the potential nucleophile attacking the adjacent carbonyls. A rate equation for the degradation of the hexapeptide has been proposed.

KEY WORDS: cyclic hexapeptide; degradation; aqueous solution; kinetics; mechanism; pH–rate profile; energetics; somatostatin.

INTRODUCTION

Inhibition of glucagon release has been proposed as a means of controlling glucose levels and may prove to be a step forward in the therapy of diabetes (1,2). Infusion experiments with somatostatin, a glucagon release inhibitor, have lent credence to this hypothesis (3). Cyclo(*N*-Me-L-Ala-L-Tyr-D-Trp-L-Lys-L-Val-L-Phe), or L-363,586 (I), is a potent cyclic hexapeptide analogue of somatostatin and a potential candidate for the treatment and control of elevated glucose levels (4). Other cyclic hexapeptide analogues of somatostatin also exhibited a longer duration of action and produced high levels of glucagon release inhibitory effects following oral administration (5,6). Compound I is about 50–100 times more potent than somatostatin as an inhibitor of insulin, glucagon, and growth hormone release (4). Studies in diabetic animals showed improved control of postprandial hyperglycemia when the compound was given orally in combination with subcutaneous insulin (7). Pharmacokinetic experiments with ^{14}C-labeled I have revealed that this drug possesses a high degree of enzymatic stability in the gastrointestinal tract, but its bioavailability following oral administration is extremely poor (1–3%) (4). Preliminary studies have suggested that this compound is sufficiently stable against aminopeptidases but undergoes chemical degradation in aqueous solution (8,9). It is a cyclic hexapeptide; however, the cyclic conformation appears to be in part due to solution instability.

Despite reports on the stability of related linear peptides of similar or larger sequences, availability of information on the stability of cyclic peptides is limited (10,11). In this report we have detailed the kinetics of degradation of compound I in aqueous solution over a wide pH range and temperature and identified the degradation products. We have attempted to identify the specific peptide linkages that are especially susceptible to degradation. Based on the amino acid sequences and the rates of formation of degradation products, mechanistic pathways for the degradation process have been suggested.

EXPERIMENTAL

Materials

Cyclo(*N*-Me-L-Ala-L-Tyr-D-Trp-L-Lys-L-Val-L-Phe), or L-363,586 (I) was kindly donated by Merck Sharp and Dohme Research Laboratories, West Point, PA. Details of the synthetic methods used in the preparation of this cyclic hexapeptide have been published elsewhere (12). All reagents used were of analytical grade.

Buffer Solutions

The following buffers were used in various pH ranges: pH 1.0–2.5, HCl; pH 3.0–5.0, acetate; pH 5.5–6.5, citrate; pH 7.0–8.0, phosphate; pH 8.2–10.5, borate; pH 11.0–12.0, NaOH. A constant ionic strength (μ = 0.5) was maintained in each buffer solution by adding an appropriate amount of sodium chloride. All the buffers were prepared at the temperature of the study. The pH measurements were made with an Accumet Model 825 MP pH meter equipped with a glass electrode (Fisher). The pH meter was standardized using certified pH 4.0 and 7.0 buffer solutions or pH 7.0 and 10.0 buffer solutions (Fisher) at the temperature of the study. Distilled, deionized water was used for the preparation of all solutions.

Kinetic Measurement

All kinetic measurements were carried out in aqueous buffer solutions at a constant ionic strength of 0.5 *M* at 60 ± 1°C unless otherwise indicated. For each data point, triplicate measurements were performed. A stock solution (1 mg/ml) of the peptide was prepared and stored in the refrigerator until further use. Each stability determination was performed by placing 1 ml of the stock solution in 10 ml of the appropriate buffer adjusted to the proper pH and ionic strength, already equilibriated to the reaction temperature, so as to produce an initial peptide concentration of 100

[1] Department of Industrial and Physical Pharmacy, School of Pharmacy and Pharmacal Sciences, Purdue University, West Lafayette, Indiana 47907.

[2] To whom correspondence should be addressed.

0724-8741/92/1000-1314$06.50/0

μg/ml. The solution was vortexed and an initial 100-μl sample was withdrawn. Subsequently 100-μl samples were removed from the reaction vessel at appropriate time intervals and immediately frozen in an acetone–dry ice mixture to quench the reaction. Upon removal of the last sample all the stored samples were thawed and peptide concentrations were determined by gradient elution HPLC using a C-18 reversed-phase column.

HPLC Analysis

Concentration of the hexapeptide remaining in solution was monitored by a reversed-phase HPLC system using a solvent delivery pump (Model Rabbit HP, Rainin Instruments, Woburn, MA) equipped with a variable UV detector (Knauer, Berlin) set at 279 nm. The column consisted of a nonpolar stationary phase (Microsorb C_{18}, 5-μm particle size, 4.6 × 250 mm; Rainin Instruments). The mobile phase was comprised of triethyl ammonium phosphate, pH 3.2 (TEAP 3.2), with a linear gradient of 27–39% (v/v) of acetonitrile over 15 min and a flow rate of 1.0 ml/min. TEAP 3.2 was prepared by adjusting phosphoric acid to pH 3.2 with triethylamine. The peak areas were calculated with an HP 3390A integrator (Hewlett-Packard, Avondale, PA). A 25-μl sample was injected onto the column. The retention time for the peptide was 11.6 min under these chromatographic conditions. Peptide loss was monitored as a function of time, as were the appearances and disappearances of various degradation products.

Identification of Degradation Products

The degradation product peaks appearing on the HPLC following acidic or alkaline treatment were selected for further analysis. Solutions (1 mg/ml) of the peptide were incubated with (i) pH 2.5, 0.1 *M* HCl solution, $\mu = 0.5$; (ii) pH 6.0, 0.1 *M* citrate buffer, $\mu = 0.5$; and (iii) pH 8.2, 0.05 *M* borate buffer, $\mu = 0.5$. Samples were withdrawn 6 hr later and stored in an acetone–dry ice mixture until further analysis.

Using the same C-18 analytical column described previously, 200-μl samples were injected onto the HPLC and eluted with the same TEAP–acetonitrile gradient. Effluents corresponding to the desired peaks were individually collected, manually, as they eluted. The separated degradation products were then individually rechromatographed using a second Rainin Microsorb C-8 column, 5 μm, 4.6 × 250 mm, but with gradients of water and acetonitrile, each containing 0.1% (v/v) trifluoroacetic acid. The water/acetonitrile mobile phase with trifluoroacetic acid gradient removed traces of impurities and allowed the degradation products to be in a volatile buffer system required for concentrating the samples suitable for amino acid (AA) sequencing analysis. The collected degradation product fractions from about five such injections were pooled and dried at room temperature using a vacuum centrifuge to remove the HPLC mobile phase. The samples were subsequently dried *in vacuo* and divided into two parts, one for amino acid sequencing and the other for fast atom bombardment mass spectrometric (FABMS) analysis.

The isolated degradation products were subjected to AA sequencing and also to FABMS for structural determination. A computer program was employed to match the mass of the observed peak with an amino acid sequence from the hexapeptide having the same molecular weight. From these results bonds labile to cleavage under different pH conditions could be identified.

Based upon the results of the kinetic experiments, the rate constants were subjected to a data fit treatment. The Enzfitter program (13) was used to fit the data to a pH–rate equation where the best-fit kinetic pK_a's were utilized to describe the observed pH–rate profile.

Molecular Modeling Study

Molecular modeling studies were performed with the program, QUANTA 2.1, and executed on a Silicon Graphics 4D120/GTX workstation. Energy minimizations were carried out using the CHARMm 2.1 energy minimizer with its default value. All structures were optimized until the energy change from one iteration to the next was less than 0.05 kcal/mol. The calculations did not take into account water molecules. The omission of solvent is a traditional limitation of computational chemistry, as its inclusion would increase the computation time dramatically.

The sequence of the hexapeptide was built using QUANTA 2.1 Sequence Builder Application. The sequence file was displayed as a structure in the Molecular Modelling Application and manipulated onscreen to be cyclic. The sequence file contained a patch to link the two ends together, but the 3D structure had to be created on-screen. The structure file thus created was subjected to minimization using CHARMm 2.1.

A conformation search was performed and the structure with minimum energy was chosen as the preferred structure. The conformation search was performed using 250 steps of Conjugate Gradient minimization for each of the *cis* and *trans* forms of the peptide bond between *N*-methyl alanine and phenylalanine. Vibrational energy was ignored and calculations were performed at a temperature of 0 K and a dielectric constant of 1.

RESULTS

Effects of pH and Buffer Concentration on Degradation

The cyclic hexapeptide (**I**) has been experimentally observed to be relatively stable against aminopeptidases but was found to be unstable in aqueous solution (8,9). The aqueous stability of **I** was studied under different pH conditions. Figure 1 illustrates a typical time course of disappearance of the hexapeptide and the appearance of the degradation products at pH 8.2 and 60°C. The degradation rate appeared to follow first-order kinetics.

The individual rate constants for the degradation of **I** in aqueous buffer solution of various pH values at 60°C and $\mu = 0.5$ have been summarized in Table I. The pH–stability profile is highly dependent on pH, with the overall rate constant showing an increasing trend with increasing alkalinity of the solutions. The rate constants obtained from the intercepts of the graphs of k_{obs} vs total buffer concentration at various pH values were used in plotting the pH–rate profile. From the pH–rate profile it could be stated that the most stable region for the peptide is between pH 4.0 and pH 5.0.

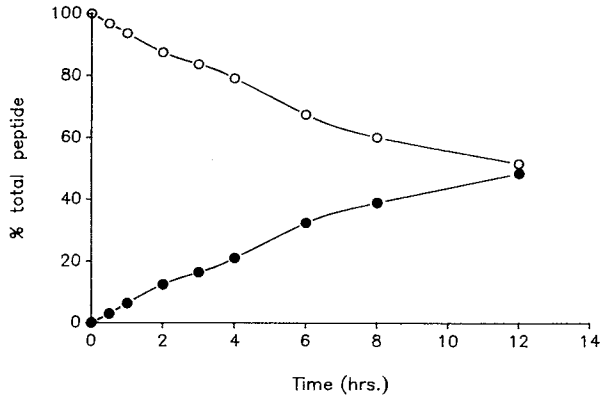

Fig. 1. Typical profile for the disappearance of the parent peptide (○) and the appearance of the cleaved product (●) at pH 8.20, 0.05 *M* borate buffer (μ = 0.5 *M*, 60°C).

The catalytic effect of the buffer was determined by measuring the rate of degradation at constant pH, ionic strength, and temperature while varying only the buffer concentration. The degree of buffer catalysis varied from buffer to buffer. The rate constants at zero buffer concentration were obtained from the intercepts of plots of k_{obs} vs total buffer concentration and have been summarized in Table II. The catalytic effect of acetate buffer on the rate of degradation is shown in Fig. 2. The peptide was relatively unstable under basic pH conditions. All of the buffers exhibited strong catalytic effects. Acetate as the catalyst shows the least influence on peptide degradation, with the nonionized acetic acid species showing the most catalytic effect of this acid/base pair. A similar trend was seen with phosphate and borate buffer systems. The slope values obtained with the various buffer systems were as follows: acetate, -1.055 M^{-1} hr^{-1}; phosphate, -1.185 M^{-1} hr^{-1}; and borate, -4.182 M^{-1} hr^{-1}. This result indicates that the k_{buffer} is associated primarily with the free acid component of all the

Table I. Observed Pseudo-First-Order Rate Constants for the Degradation of L-363,685 in Aqueous Buffer Solutions of Various pH Values (60°C, μ = 0.5 *M*)

pH	Buffer conc. (*M*)	k_{obs} (hr^{-1})	(±SD)
1.0	0.05	41.61×10^{-3}	(0.003)
	0.1	1.67×10^{-3}	(0.002)
3.0	0.01	4.61×10^{-4}	(0.0007)
	0.03	8.7×10^{-4}	(0.003)
	0.05	0.004	(0.0003)
4.7	0.01	9.00×10^{-5}	(0.0001)
	0.025	4.31×10^{-4}	(0.0014)
	0.05	2.21×10^{-3}	(0.0031)
5.0	0.01	1.92×10^{-4}	(0.0051)
	0.05	2.69×10^{-3}	(0.0021)
6.0	0.01	3.55×10^{-3}	(0.0011)
	0.05	6.11×10^{-3}	(0.002)
	0.1	7.75×10^{-3}	(0.0031)
7.0	0.01	5.08×10^{-3}	(0.0031)
	0.05	7.91×10^{-3}	(0.013)
	0.1	9.31×10^{-3}	(0.0021)
7.4	0.01	7.01×10^{-3}	(0.0031)
	0.05	7.64×10^{-3}	(0.004)
	0.1	8.42×10^{-3}	(0.006)
8.2	0.01	2.21×10^{-2}	(0.006)
	0.05	1.28×10^{-2}	(0.0011)
	0.1	2.5×10^{-2}	(0.013)
9.0	0.01	5.00×10^{-2}	(0.036)
	0.05	4.93×10^{-2}	(0.04)
	0.1	5.7×10^{-2}	(0.11)
10.0	0.005	0.1025	(0.27)
	0.01	0.094	(0.224)
	0.05	0.095	(0.072)
10.5	0.005	0.11	(0.032)
	0.01	0.1875	(0.24)
	0.025	0.1625	(0.101)
	0.05	0.1703	(0.024)
11.0	0.01	0.130	(0.06)
	0.05	0.162	(0.08)

Table II. The Rate Constants of Degradation of L-363,586 at Zero Buffer Concentration (k_o) at μ = 0.5 *M*, 60°C

pH	k_o (hr^{-1})
1.0	1.585×10^{-3}
1.5	9.772×10^{-4}
2.5	2.818×10^{-4}
3.0	1.585×10^{-4}
3.2	1.625×10^{-4}
4.0	6.025×10^{-5}
4.5	5.495×10^{-5}
4.7	4.785×10^{-5}
5.0	9.772×10^{-5}
5.5	1.905×10^{-4}
6.0	2.238×10^{-3}
6.5	3.89×10^{-3}
7.0	5.011×10^{-3}
7.4	6.338×10^{-3}
7.6	6.607×10^{-3}
8.0	8.127×10^{-3}
8.2	0.013
8.6	0.022
9.0	0.038
9.2	0.045
9.5	0.079
10.0	0.099
10.5	0.116
11.0	0.125
12.0	0.246

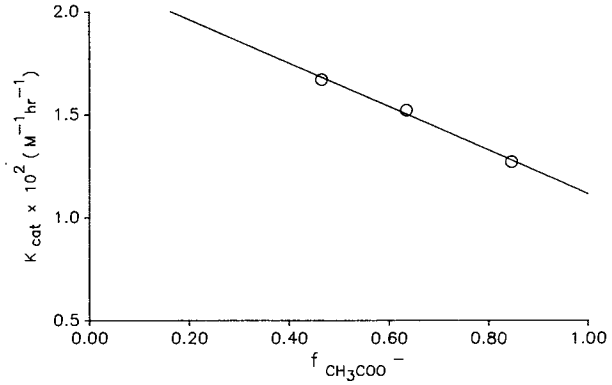

Fig. 2. Dependence of catalytic rates of L-363,586 degradation on fraction of acetate anion (○) at 60°C and μ = 0.5 *M*.

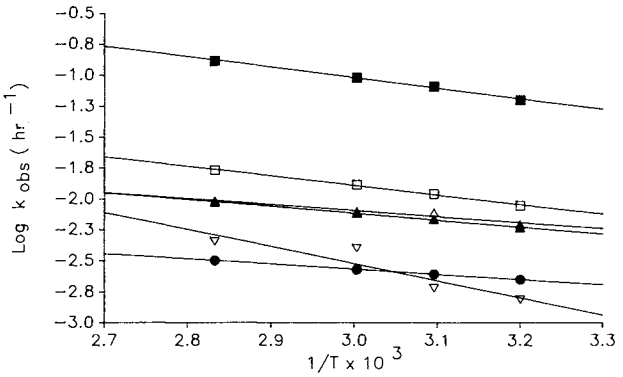

Fig. 3. Arrhenius plot for L-363,586 at different pH values (buffer concentration = 0.5 *M*, μ = 0.5 *M*). pH 3.2 (▽); pH 5.0 (●); pH 7.0 (△); pH 7.4 (▲); pH 8.2 (□); pH 10.0 (■).

buffers, suggesting a possible proton donation in the transition state complex formation.

Effect of Temperature on Degradation

Degradation of the peptide was studied at pH 3.2, 5.0, 7.0, 7.4, 8.2, and 10.0 (μ = 0.5) and at four different temperatures between 37 and 70°C (±1°C). The rates of reaction, as expected, increased with an increase in temperature. From the Arrhenius plot (Fig. 3) it was possible to calculate the activation energies. The enthalpies and entropies of activation were calculated using an Eyring plot (Fig. 4) (14,15). The thermodynamic parameters thus calculated are summarized in Table III. The free energy associated with the reaction seems to be governed more by the entropic process rather than the enthalpy associated with the bond breaking as can be seen from the large negative contribution of ΔS.

Identification of Degradation Products

Amino acid sequencing of the various degradation products collected from the HPLC elutions suggests an initial ring opening to yield a linear peptide which has all six amino acids in the same sequence as the parent peptide. This observation suggests that the amide linkage between methylalanine and phenylalanine residues is always cleaved first to generate a stable intermediate irrespective of the pH conditions. Further sequencing data reveal that under both acidic and alkaline conditions, cleavages also occur at both the peptide linkages alpha to the tryptophan residue, to yield

(a) Me-Ala-Tyr and Trp-Lys-Val-Phe and
(b) Me-Ala-Tyr-Trp and Lys-Val-Phe.

To confirm these data the same fractions were subjected to FABMS, and the results were in agreement with the AA sequencing analysis (Table IV). The entire degradation scheme is illustrated in Scheme I.

Studies are in progress to try to verify the nature of the peptide bond (*cis* versus *trans*) at the site of initial cleavage using NMR techniques. A combination of techniques such as NMR and FTIR, along with the fragments identified thus far, should help in justifying the scheme outlined.

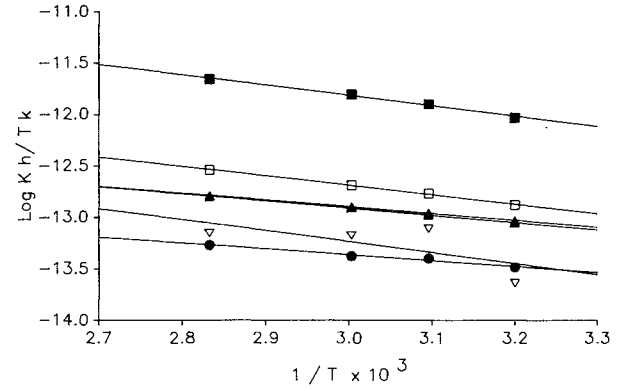

Fig. 4. Eyring plot for L-363,586 at different pH values (buffer concentration = 0.5 *M*, μ = 0.5 *M*). pH 3.2 (▽); pH 5.0 (●); pH 7.0 (△); pH 7.4 (▲); pH 8.2 (□); pH 10.0 (■).

Table III. Thermodynamic Parameters Calculated for the Degradation of L-363,586 in Aqueous Solution

pH	E_a (kcal/mol)	ΔH (kcal/mol)	ΔS (cal/mol deg)
3.2	6.31	4.92	−46.24
5.0	1.93	2.61	−53.72
7.0	2.24	3.05	−50.27
7.4	2.53	3.23	−49.78
8.2	3.55	4.22	−45.80
10.0	3.93	4.62	−40.57

DISCUSSION

The results obtained from the fitting of the rate data using the Enzfitter program suggested that the two ionization constants for the peptide are pK_1 = 5.797 and pK_2 = 8.859. The first pK_a can be assigned to the alpha COOH terminus of the linear peptide, and the latter one to the Tyr-OH (16). The unusually high pK_a of the carboxy terminus could be due to some neighboring structural effects shielding the carboxyl group or could be the kinetic pK_a representing change in the rate-determining step (17).

The pH dependence of the degradation of the hexapeptide (Pep) as a function of time can be described mathematically by considering the following possible reactions.

Reaction		Rate constant	
$Pep^+ + H^+$	→ products	k_1	(1)
$Pep^{+-} + H^+$	→ products	k_2	(2)
$Pep^{+-} + H_2O$	→ products	k_3	(3)
$Pep^{+--} + H_2O$	→ products	k_4	(4)
$Pep^{+--} + OH^-$	→ products	k_5	(5)

Table IV. Fragment Identification Using Mass Spectrometric and Amino Acid Sequence

Fragment no.	Molecular weight (M + 1)	Fragment sequence
I	809.5	MeAla-Tyr-Trp-Lys-Val-Phe
II	737.5	Trp-Lys-Val-Phe
III	277.3	Me-Ala-Tyr
IV	502.5	Lys-Val-Phe
V	490.4	Me-Ala-Tyr-Trp

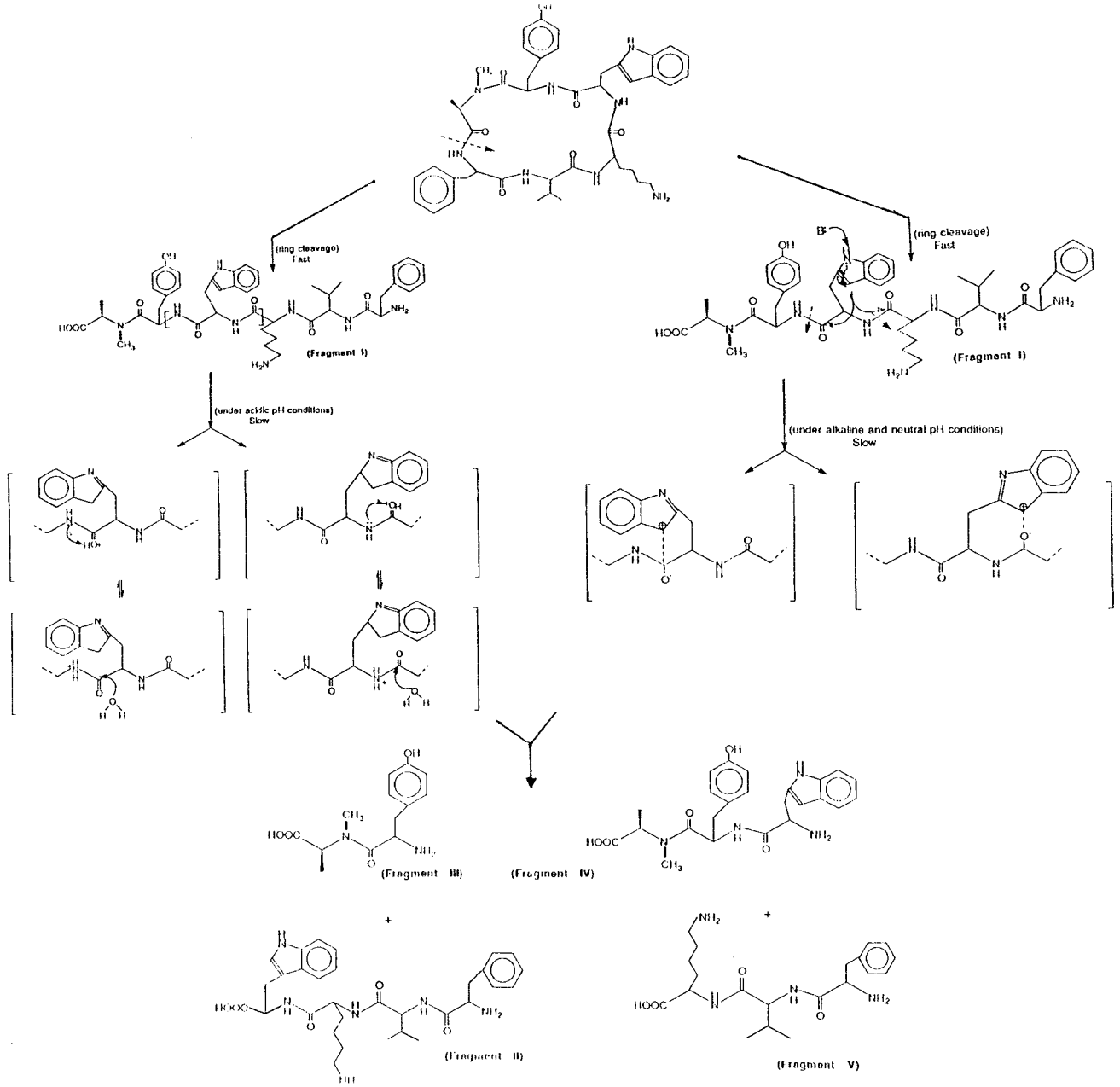

Scheme I. Scheme for the degradation of the hexapeptide under different pH conditions.

The rate constants k_1 and k_5 have been evaluated from the intercepts at the pH extremes. The other microscopic rate constants have been obtained from computer fit by iterating the experimental data points into Eq. (6). The individual rate constants summarized in Table V were determined by curve fitting the data. From the values obtained it is evident that that hydroxide-catalyzed reaction (k_5) is three orders of magnitude higher than the acidic reaction (k_1). Also, from the values of k_2 and k_3, which differ by one order of magnitude, it appears that the water-catalyzed reaction of the zwitterionic form is slower than its acidic reaction rate. The value of k_4 is negligible and was disregarded in the proposed rate equation. The line representing the theoretical curve shows a fair agreement with the observed experimental values. Within the pH range of 3.5 and 10.0, the rate equation (6) derived on the basis of the two ionizations fit the experimental data, as shown in Fig. 5.

Proposed Rate Equation

$$k_0 = \frac{k_1[H^+]^2 + k_2[H^+] + k_3K_1 + k_5K_2}{[H^+]^2 + [H^+]K_1 + K_1K_2} \qquad (6)$$

The sequencing data suggest that the cyclic structure first undergoes rapid ring opening to yield a linear molecule which then degrades to generate further fragments. The most susceptible peptide bond under any given pH condition appears to be the one between methylalanine and phenylala-

Table V. Rate Constants Determined by Fitting the Data According to Eq. (6)

k_1	$5.99 \times 10^{-3}\ M^{-1}\ hr^{-1}$
k_2	$1.27 \times 10^{-3}\ hr^{-1}$
k_3	$3.39 \times 10^{-4}\ hr^{-1}$
k_4	$3.33 \times 10^{-7}\ hr^{-1}$
k_5	$12.59\ M^{-1}\ hr^{-1}$

nine. The subsequent cleavage of the linear peptide at the tryptophan residue, between either tryptophan–tyrosine or tryptophan–lysine, probably follows different mechanisms under acidic and alkaline conditions. The suggested mechanism of the degradation involves a charged intermediate. Solvation (i.e., hydration) of this charged transition-state intermediate accounts for the large entropy loss for the transition state. Clearly, the librational entropy increase upon cleavage of the cyclic form to the linear peptide renders the reaction irreversible. Hence, the degradation of the cyclic peptide itself is rate limited by the entropy of the solvation of the charged intermediate and this is evidenced by the large negative entropy values. As represented in Scheme I, in the acidic pH range the cleavage requires the protonation of the amide oxygen close to the indole ring, where it is facilitated by the acidic components of the buffer.

In the neutral to alkaline pH range the presence of a nucleophilic carbanion (as in the C_3 position of the indole structure) may catalyze the cleavage of adjacent amide bonds (Scheme I). The nucleophilic carbanion may attack any of the adjacent amide carbonyl carbons, resulting in either a five- or a six-membered ring in the transition state. When the point of attack is the amide bond between tyrosine and tryptophan, the resulting products are Me-Ala-Tyr and Trp-Lys-Val-Phe, whereas breakdown of the amide bond between tryptophan and lysine generates Me-Ala-Tyr-Trp and Lys-Val-Phe.

The energy minimization computation study (Figs. 6a and b) suggests that the cyclic nature of the peptide causes the peptide bond between *N*-methyl alanine and phenylalanine to have a *cis* configuration, presumably because of a *N*-methyl locking arrangement of the peptide bond in the *N*-methyl alanyl residue. Studies carried out with another analogue, where proline replaced the *N*-methyl alanine residue, indicated similar NMR features and nearly identical CD spectra, suggesting a close similarity in conformation between the two in solution and the possible existence of a *cis* peptide bond (18,19). As a result, this bond is strained and has a higher internal energy of ~45 kcal/mol, as compared to the normal *trans* configuration, with an internal energy of ~41 kcal/mol. It can be proposed that in order to relieve the strain, the ring opens up to form the linear peptide. The degradation reaction appears to proceed via a stable intermediate of the linear peptide. Transformation of the cyclic peptide to linear peptide is fast because of the low-energy barrier due to the strain in the *cis* peptide bond. The breakdown of the intermediate by nucleophilic attack of the tryptophanyl residue has a high-energy barrier as shown in Table III. This is the slower of the two-step degradation process and, as such, appears to be the rate-limiting step. The bond energy and nature of bonding between the methylalanine and the phenylalanine residues must be experimentally determined to give credence to this theory that a *cis* peptide bond exists between these two amino acid residues.

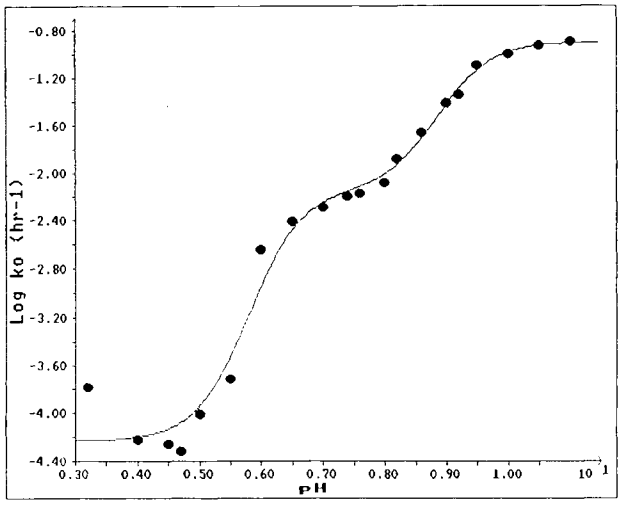

Fig. 5. Simulated pH–rate profile compared to that of the data obtained experimentally. Experimental data (●), curve fitted according to Eq. (6).

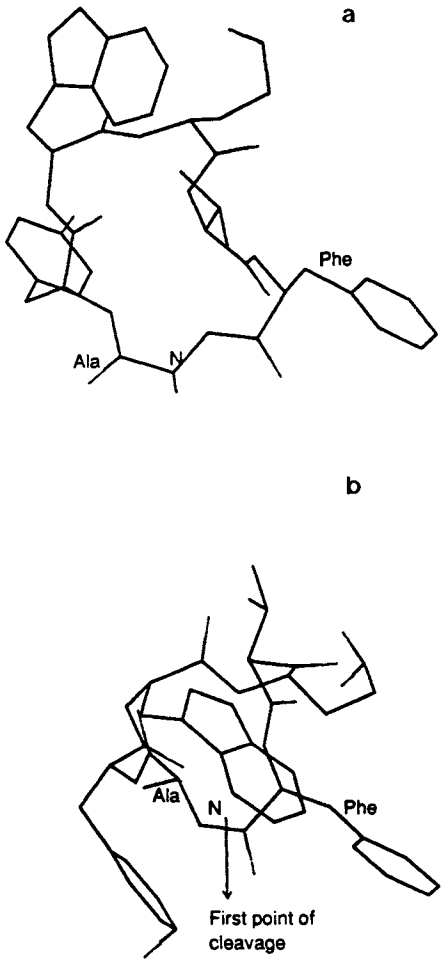

Fig. 6. (a) Structural representation of the *trans* configuration of the peptide. (b) Structural representation of the cis configuration of the peptide.

This could possibly be done using two-dimensional NMR spectroscopy where any *cis*-to-*trans* transition occurring in solutions under different pH conditions could be followed. This information will provide a better understanding of the mechanism, thereby enabling us to design molecules with greater stability.

Studies are presently under way to verify the nature of the peptide bond between methylalanine and phenylalanine residues using two-dimensional NMR spectroscopy, which might help us to understand better the chemical instability of an otherwise enzymatically stable cyclic peptide. The solution instability could provide a reason for the poor oral bioavailability of the compound and also may provide a rationale for suitable chemical modifications without causing any significant loss of bioactivity of such cyclic peptides.

ACKNOWLEDGMENTS

The authors would like to thank Dr. Daniel F. Veber of the Merck Sharp and Dohme Research Laboratories for his generous gift of the hexapeptide. The authors are grateful to Professor David Smith of the Medicinal Chemistry and Pharmacognosy Department, Purdue University, for assistance with the FABMS analyses of the fragments. The authors would also like to thank Mary Woenker for helping with the amino acid sequencing analysis, Anthony Gilleto for providing help with use of the Enzfitter software, and Betsy Leverett for providing help with computer modeling.

This investigation was supported in part by a Young Investigator Award from the American Association of Pharmaceutical Scientists (A.K.M.) and a Merck Faculty Development Award (A.K.M.).

REFERENCES

1. R. H. Unger. Glucagon physiology and pathophysiology. *N. Engl. J. Med.* 285:443–448 (1971).
2. J. E. Gerich. Somatostatin modulation of glucagon secretion and its importance in human glucose homeostasis. *Metabolism* 27:1283–1286 (1978).
3. J. E. Gerich, T. A. Schultz, S. B. Lewis, and J. H. Karam. Clinical evaluation of somatostatin as a potential adjunct to insulin in the management of diabetes mellitus. *Diabetologia* 13:537–544 (1977).
4. D. F. Veber, R. Saperstein, R. F. Nutt, R. M. Freidinger, S. F. Brady, P. Curley, D. S. Perlow, W. J. Paleveda, C. D. Colton, A. G. Zacchei, D. J. Tocco, D. R. Hoff, R. L. Vandlen, J. E. Gerich, L. Hall, L. Mandarino, E. H. Cordes, P. S. Anderson, and R. Hirschmann. A super active cyclic hexapeptide analog of somatostatin. *Life Sci.* 34:1371–1378 (1984).
5. D. F. Veber, F. W. Holly, W. J. Paleveda, R. F. Nutt, S. J. Bergstrand, M. Torchiana, M. S. Glitzer, R. Saperstein, and R. Hirschmann. Conformationally restricted bicyclic analogs of somatostatin. *Proc. Natl. Acad. Sci. USA* 75:2636–2640 (1978).
6. D. F. Veber, R. M. Freidinger, D. S. Perlow, W. J. Paleveda, F. W. Holly, R. G. Strachan, R. F. Nutt, B. H. Arison, C. Homnick, W. C. Randall, M. S. Glitzer, R. Saperstein, and R. Hirschmann. A potent cyclic hexapeptide analogue of somatostatin. *Nature* 292:55–58 (1981).
7. W. Bauer, U. Briner, W. Doetner, R. Haller, R. Huguenin, P. Marbach, T. J. Petcher, and J. Pless. A potent and long acting somatostatin analog of somewhat larger molecular size also has been reported to be of sufficient interest to warrant human evaluation. *Life Sci.* 31:1133–1140 (1982).
8. C. R. Gardner, S. Selk, M. Cortese, and T. Higuchi. In-situ peptide absorption studies—uptake, binding or metabolism? Presented at the Higuchi Research Seminar, 17th Annual Meeting, Lake Ozark, MO, March 1986.
9. C. R. Gardner. Gastrointestinal barrier to oral drug delivery. In R. T. Borchardt, A. J. Repta, and V. J. Stella (eds.), *Directed Drug Delivery,* Humana Press, Clifton, NJ, 1985, pp. 61–81.
10. K. Patel and R. T. Borchardt. Chemical Pathways of Peptide degradation. II. Kinetics of Deamidation of an Asparaginyl Residue in a model Hexapeptide. *Pharm. Res.* 7:703–711 (1990).
11. M. C. Manning, K. Patel, and R. T. Borchardt. Stability of protein pharmaceuticals. *Pharm. Res.* 6:903–918 (1989).
12. S. F. Brady, R. M. Freidinger, W. J. Paleveda, C. D. Colton, C. F. Homnick, W. L. Whitter, P. Curley, R. F. Nutt, and D. F. Veber. Large scale synthesis of a cyclic hexapeptide analogue of somatostatin. *J. Org. Chem.* 52:764–769 (1987).
13. Enzfitter: A non-linear regression analysis program for the IBM PC by R. J. Leatherbarrow.
14. H. Eyring. Quantum mechanics and chemical reactions. *Chem. Rev.* 10:103–110 (1965).
15. H. Eyring. The activated complex and the absolute rate of chemical reactions. *Chem. Rev.* 17:65–69 (1935).
16. E. Tanford. The interpretation of hydrogen ion titration curves of proteins. *Adv. Protein Chem.* 17:69–165 (1962).
17. A. Fersht. The pH dependence of enzyme catalysis. In *Enzyme Structure and Mechanism,* 2nd ed., W. H. Freeman, New York, 1985, pp. 155–175.
18. D. F. Veber. Peptides: Synthesis, structure, function. In D. H. Rich and E. Gross (eds.), *Proceedings of the Seventh American Peptide Symposium,* Pierce Chemical Co., Rockford, IL, 1981, pp. 685–694.
19. B. H. Arison, R. Hirschmann, and D. F. Veber. Inferences about the conformation of somatostatin at a biologic receptor based on NMR studies. *Bioorg. Chem.* 7:447–451 (1978).